Available online at www.sciencedirect.com
ScienceDirect
Ceramics International 38S (2012) S627–S630
CERAMICS INTERNATIONAL
www.elsevier.com/locate/ceramint

Epitaxial growth and electrical transport property of artificial $LaNiO_3/LaAlO_3$ superlattices

A.N. Jang, S.K. Seung, K.H. Choi, J.H. Song *

Department of Physics, Chungnam National University, Daejeon 305-764, Republic of Korea

Available online 27 May 2011

Abstract

We successfully grew epitaxial $LaNiO_3$(1 u.c.)/$LaAlO_3$(1 u.c.) superlattices on single crystal $LaAlO_3$ (0 0 1) substrates using pulsed laser deposition method. Specular RHEED intensity oscillations were repeated continuously throughout the entire growth. Large angle θ–2θ X-ray scans show only the peaks from the superlattices and substrates. These results verify the highly qualified crystal structure of the superlattices. The temperature dependence of the resistivity exhibits a semiconducting behavior in the entire temperature range studied. These observations indicate that the semiconducting characteristics of the superlattice are attributed to the radical alteration of the electronic structure of the NiO_2 layers.

Keywords: A. Films; C. Electrical conductivity; D. Perovskites; Superlattices

1. Introduction

Due to recent advances in the synthesis of complex oxide thin films, building up perovskite-based hetero-structures with abrupt interface and artificial superlattices becomes an emerging field because expected their exotic properties can open up new possibilities of next generation devices [1–4]. As an example for the hetero-structure, unusual quantum-meta phase is stabilized at the interface in $LaAlO_3/SrTiO_3$ heteroepitaxial thin film as reported by Ohtomo and Hwang [5] and has attracted enormous attention due to the possibilities of interface-controlled devices [6–9]. The alternate stacking of different MO_2 layers in perovskite superlattice structure provides another approach for novel material through the artificial atomic order that have not been achieved in the bulk. The representative example is the realization of ferromagnetic spin order in $[LaCrO_3(1\text{ u.c.})/LaFeO_3(1\text{ u.c.})]_N$ superlattice grown on $SrTiO_3$ (1 1 1) substrate [1]. The exploring of non-cupurate-based superconductivity in $[LaNiO_3(1\text{ u.c.})/LaAlO_3(1\text{ u.c.})]_N$ is one of the examples of such efforts with the aim of new novel materials [10]. Toward this goal, delicate synthesis technology in stacking the MO_2 layers is of fundamental importance.

In this paper, we report on the growth of $[LaNiO_3(1\text{ u.c.})/LaAlO_3(1\text{ u.c.})]_{60}$ superlattices and their structural and electrical-transport properties. Of particular interests are the expitaxial stabilization of $LaNiO_3$(LNO) and $LaAlO_3$(LAO) layers in the form of superlattice and their electronic characteristics. To clarify the effect of oxygen vacancies in the superlattices on the electronic characteristics, we have post-growth annealed the superlattice samples carefully and investigated the changes of the temperature dependencies of the resistivity.

2. Experimental

Epitaxial LNO/LAO superlattices were grown on TiO_2-terminated LAO single crystal substrates by pulsed laser deposition with *in situ* monitoring by reflection high energy electron diffraction (RHEED, Pascal RHD-307-2 Japan) using a KrF excimer laser. To obtain flat surface structures with straighten terrace steps, all substrates used were pre-annealed at 950 °C in an oxygen environment of 5×10^{-6} Torr for at least 30 min followed by lowering to the growth temperature of 750 °C, as measured by an external optical pyrometer. A single crystalline LAO and sintered stoichiometric poly crystalline LNO pellet were used as targets. The laser fluence and

* Corresponding author. Tel.: +82 42 8215455; fax: +82 42 8228011.
E-mail address: songjonghyun@cnu.ac.kr (J.H. Song).

0272-8842/$36.00
doi:10.1016/j.ceramint.2011.05.112

repetition rate were fixed to 0.4 J/cm^2 and 2 Hz, respectively. The oxygen partial pressure P_{O_2} was kept to 1 mTorr throughout the growth. After growth the samples were cooled to room temperature in $P_{O_2} = 1$ mTorr, the same oxygen environment to during the growth. These as-grown samples were subjected to an *ex situ* post-growth annealing in a quartz tube for 5 h under flowing high purity O_2 gas (99.995%) at 600 °C to remove any possibly driven oxygen vacancies during the growth. Electrical resistivity was measured by the conventional four-probe method using Physical Property Measurement System (PPMS, Quantum Design U.S.A.).

3. Results and discussion

Fig. 1(a) shows the designed crystal structure of LNO(1 u.c.)/LAO(1 u.c.) superlattice. To realize the design, successive layers of AlO_2, LaO, NiO_2 and LaO were grown by turns with a total thickness of ∼47 nm, resulting in the atomic order of Al–O–Ni along the surface normal direction of the films. To control the sequence of the atomic layers, we monitored specular RHEED intensity on time throughout the entire growth. After the growth of AlO_2–LaO layers with AlO_2 termination, as indicated by a recovered specular intensity after damping, the LAO single crystal target was exchanged to LNO to grow subsequent NiO_2–LaO layers. For all LAO and LNO growths, the recovered and then saturated behavior of the specular RHEED intensity in a period of oscillation is believed to originate from the complete growth of MO_2 layers if we consider the two facts: (i) MO_2 termination is favored for both LNO and LAO growth [11,12] and (ii) signal implying the conversion of the terminating atomic layer as reported by Rijnders et al. [13] in the growth of $SrRuO_3$ is not observed at here.

Just after the subsequent growth of LNO after LAO, the intensity enhanced rapidly followed by a clear oscillation. At here it should be noted the relative difference in the recovered intensity after the each growth of LAO and LNO. The typical RHEED patterns after the growth of LAO (Fig. 1(e)) are relatively darker than those after the growth of LNO (Fig. 1(d)). These observations indicate that the surface structure of AlO_2 layer after the growth of LAO is relatively rough compared to that of NiO_2 layer after the growth of LNO. The relatively rough AlO_2 surface is understandable if we consider the rhombohedral crystal structure of LAO and the textured surface of the single crystal which can be easily observed even by naked eyes. For the observed rapid enhancement of the RHEED intensity just after the growth of LNO, we suggest a flattened surface by the subsequently grown LaO layer while the followed single oscillation is attributed to the growth of flat NiO_2 layer. Fig. 1(c) and (d) is observed RHEED patterns of LAO single crystal substrate taken before growth and superlattice after the entire growth with NiO_2 layer termination, respectively. The bright specular spot and streaky RHEED patterns in Fig. 1(d) which are similar to that in Fig. 1(c) indicate the flat surface even after thick (∼47 nm) growth.

Fig. 2(a) shows the X-ray diffraction data for the grown [LNO(1 u.c.)/LAO(1 u.c.)]$_{60}$ superlattice sample. Large angle θ–2θ X-ray scans (10–80°) show only the diffraction peaks from the substrate and superlattice. These results contrast with the X-ray diffraction data for the single layered LNO thin film grown on LAO (0 0 1) substrate with the same growth parameter showing the additional peaks from the secondly phase and also other crystal orientations (the data is not shown at here). These observations indicate that the growth of LNO is epitaxial stabilized through the form of LNO/LAO superlattice. If we define the unit cell of the superlattice to double-perovskite La_2AlNiO_6 (LANO), the peaks at ∼22.7°, 46.4° and 72.5° are

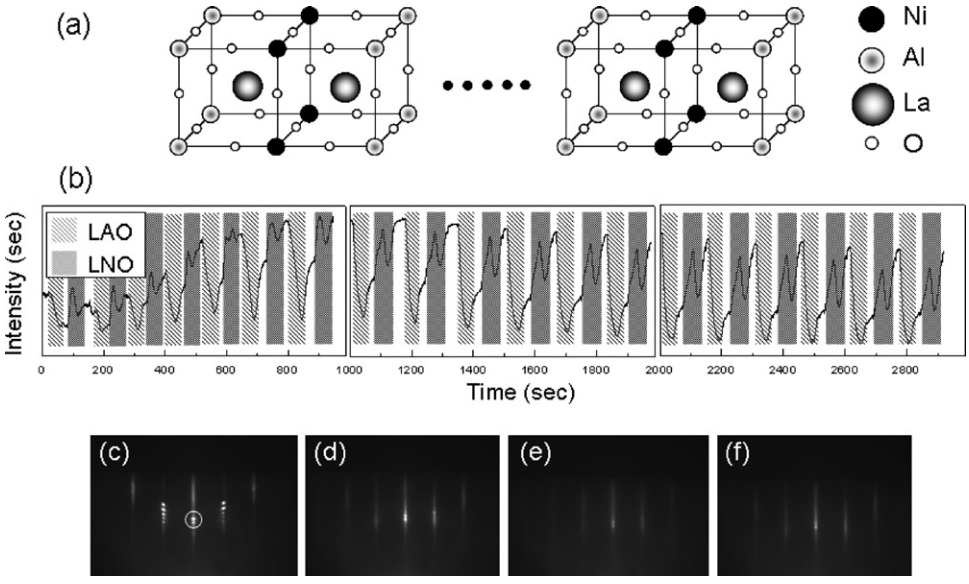

Fig. 1. (a) Crystal structures of $LaNiO_3$/$LaAlO_3$ superlattice with alternating AlO_2 and NiO_2 planes. (b) Specular RHEED intensity oscillations observed during growth of the superlattice. As shown in the inset the slashed and shaded areas correspond to the growth of $LaAlO_3$ and $LaNiO_3$ layers, respectively. Observed RHEED patterns for (c) the TiO_2 layer terminated $LaAlO_3$ substrate, (d) after the growth of $LaNiO_3$, (e) $LaAlO_3$ layers, and (f) after the entire growth. The specular spot is in the white circle at (c). The growth was terminated with a LNO deposition.

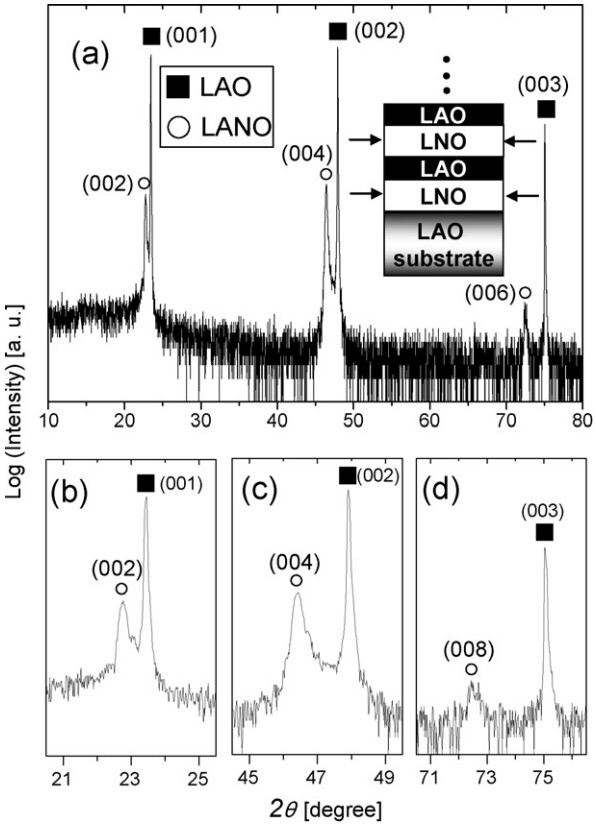

Fig. 2. The θ–2θ X-ray diffraction data for La_2NiAlO_6 superlattice grown on $LaAlO_3$ substrate. Open circles and filled squares signify the peaks from La_2NiAlO_6 superlattice and from $LaAlO_3$ substrate, respectively. (b)–(d) Magnified views of each peak.

from the (0 0 2), (0 0 4) and (0 0 6) crystal planes of the double-perovskite, respectively. Note that any satellite peaks are not observed which may appear due to the deviated periodicity from 1 u.c./1 u.c. These results confirm that the superlattices with alternating AlO_2 and NiO_2 layers are successfully grown.

The *c*-axis lattice constant of the double-perovskite unit cell extracted from the X-ray diffraction data is 0.7820 nm, the larger than the value (0.7627 nm) deduced from the pseudo-cubic lattice constant of LNO ($a = 0.3838$ nm) [14] and LAO ($a = 0.3789$ nm) [5] in the bulk. These observations indicate that LNO layers in the superlattices are elongated along the *c*-axis due to the bi-axial strain applied from the LAO substrate as well as adjacent AlO_2 layers. The observed shoulders at the right side of the peaks from LANO which can be observed at the zoomed view in Fig. 2(b)–(d) are attributed to the volume fraction in the superlattices with slightly smaller *c*-axis lattice constant than the majorly observed phase. These structural changes are thought to be caused by a relaxation of the bi-axial strain at the thick side of the superlattices.

Fig. 3 shows the temperature dependencies of the resistivity for the as-grown and post-growth annealed superlattices. The post-growth annealing was carried out carefully at 600 °C; this temperature is believed to high enough in removing the possible oxygen vacancies in LNO layers as reported by Wang et al. [15] but further lower than the growth temperature (750 °C) and therefore may avoid any structural change by annealing. As

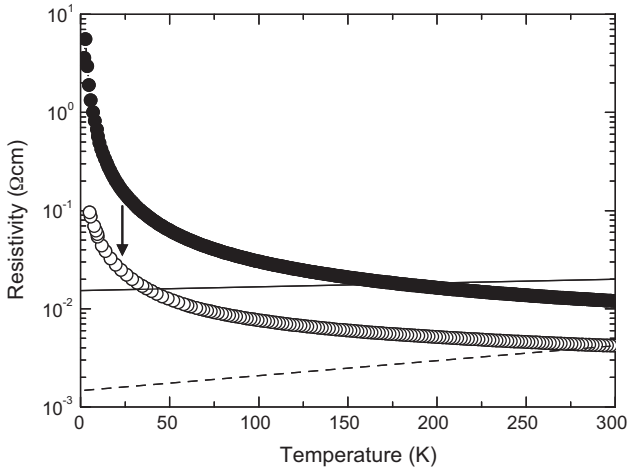

Fig. 3. Temperature dependency of resistivity for as-grown (filled circles) and post-growth annealed (open circles) superlattice samples studied. The solid (dashed) line is a mimic data for the single layered $LaNiO_3$ thin film grown at 0.5 (30) mTorr oxygen partial pressure followed by cooling in 1 atm of oxygen [12].

shown, the temperature dependency of the resistivity of the as-grown superlattice exhibits semiconducting behavior with an upturn at low temperature. This semiconducting behavior is not changed after post-growth annealing while only the value of the resistivity is decreased as shown, indicating the existence of oxygen vacancies in the as-grown superlattice. From these observations, we can rule out oxygen vacancies as an origin of the observed semiconducting behavior of the superlattices. To understand the microscopic origin of this semiconducting behavior, further study is needed.

4. Conclusions

We grew epitaxial $[LNO(1\text{ u.c.})/LAO(1\text{ u.c.})]_{60}$ superlattices on LAO single crystal substrates using pulsed laser deposition. The layer-by-layer growth mode with clear specular RHEED intensity oscillations is observed to the end of the growth. The large angle θ–2θ X-ray scans show only the peaks from the superlattices and substrates without any indication of the deviated periodicity from 1 u.c./1 u.c. These results confirm the high quality of the superlattices. Even the value of the resistivity is decreased after post-growth annealing, the semiconducting behavior in the temperature dependency of the resistivity is not changed. These experimental observations indicate that the observed semiconducting characteristics of the superlattices are from the radical alteration of the electronic structure of LNO layers in the superlattices.

Acknowledgements

This research was supported by Basic Science Research Program through the National Research Foundation of Korea (NRF) funded by the Ministry of Education, Science and Technology (2009-0071272) and also was supported by the Korea Science and Engineering Foundation (KOSEF) grant

funded by the Ministry of Education, Science and Technology (2008-0059220).

References

[1] K. Ueda, H. Tabata, T. Kawai, Ferromagnetism in $LaFeO_3$–$LaCrO_3$ superlattices, Science 280 (1998) 1064–1066.
[2] C.H. Ahn, K.M. Rabe, J.-M. Triscone, Ferroelectricity at the nanoscale: local polarization in oxide thin films and heterostructures, Science 303 (2004) 488–491.
[3] A. Ohtomo, D.A. Muller, J.L. Grazul, H.Y. Hwang, Artificial charge-modulation in atomic-scale perovskite titanate superlattices, Nature 419 (2002) 378–380.
[4] H.N. Lee, H.M. Christen, M.F. Chisholm, C.M. Rouleau, D.H. Lowndes, Strong polarization enhancement in asymmetric three-component ferroelectric superlattices, Nature 433 (2005) 395–399.
[5] A. Ohtomo, H.Y. Hwang, A high-mobility electron gas at the $LaAlO_3$/$SrTiO_3$ heterointerface, Nature 427 (2004) 423–426.
[6] S. Thiel, G. Hammerl, A. Schmehl, C.W. Schneider, J. Mannhart, Tunable quasi-two-dimensional electron gases in oxide heterostructures, Science 313 (2006) 1942–1945.
[7] A.D. Caviglia, S. Gariglio, N. Reyren, D. Jaccard, T. Schneider, M. Gabay, S. Thiel, G. Hammerl, J. Mannhart, J.-M. Triscone, Electric field control of the $LaAlO_3$/$SrTiO_3$ interface ground state, Nature 456 (2008) 624–627.
[8] C. Cen, S. Thiel, G. Hammerl, C.W. Schneider, K.E. Andersen, C.S. Hellberg, J. Mannhart, J. Levy, Nanoscale control of an interfacial metal–insulator transition at room temperature, Nature Materials 295 (2002) 298–302.
[9] W. Siemons, G. Koster, H. Yamamoto, W.A. Harrison, G. Lucovsky, T.H. Geballe, D.H.A. Blank, M.R. Beasley, Origin of charge density at $LaAlO_3$ on $SrTiO_3$ heterointerfaces: possibility of intrinsic doping, Physical Review Letters 98 (196802) (2007) 1–4.
[10] J. Chaloupka, G. Khaliullin, Orbital order and possible superconductivity in $LaNiO_3$/$LaMO_3$ superlattices, Physical Review Letters 100 (016404) (2008) 1–4.
[11] M. Kawasaki, K. Takahashi, T. Maeda, R. Tsuchiya, M. Shinohara, O. Ishiyama, T. Yonezawa, M. Yoshimoto, H. Koinuma, Atomic control of the $SrTiO_3$ crystal surface, Science 266 (1994) 1540–1542.
[12] K. Tsubouchi, I. Ohkubo, H. Kumigashira, Y. Matsumoto, T. Ohnishi, M. Lippmaa, H. Koinuma, M. Oshima, Epitaxial growth and surface metallic nature of $LaNiO_3$ thin films, Applied Physics Letters 92 (262109) (2008) 1–3.
[13] G. Rijnders, D.H.A. Blank, J. Choi, C.B. Eom, Enhanced surface diffusion through termination conversion during epitaxial $SrRuO_3$ growth, Applied Physics Letters 84 (2004) 505–507.
[14] A. Wold, B. Post, E. Banks, Rare earth nickel oxides, Journal of the American Ceramic Society 79 (1957) 4911–4913.
[15] Z.J. Wang, T. Kumagai, H. Kokawa, Microstructure and electrical properties of lanthanum nickel oxide thin films deposited by metallo-organic decomposition method, Journal of Crystal Growth 290 (2006) 161–165.